九州大学大学院総合理工学府報告
第 45 巻 第 1 号 1-6 頁 令和 5 年 9 月

Engineering Sciences Reports, Kyushu University
Vol. 45, No. 1, pp. 1-6, SEP, 2023

Cellular characterization of hiPS-CMs cultured on PMEA analogous polymers with different bound water content

Hiroko KURITA,[*1†] Shingo KOBAYASHI,[*2] Takahisa ANADA,[*2,3]
Masaru TANAKA[*2,3] and Mitsugu TODO[*4,5]
[†]E-mail of corresponding author: kurita.hiroko.087@s.kyushu-u.ac.jp

(Received March 22, 2023, accepted April 4, 2023)

In recent years, human iPS cell-derived cardiomyocytes (hiPS-CMs) have attracted much attention in the arena of regenerative therapies. However, hiPS-CMs are known to be immature and have lower contractility than the adult heart. In this study, we investigated the effect of material properties of scaffold surfaces on hiPS-CMs with the aim of improving the contractility of hiPS-CMs. PMEA analogs with varying surface-bound water content, which affect cell adhesion/proliferation behavior, were selected as scaffold materials to coat PET substrates. The cell characteristics of the hiPS-CMs seeded on the scaffolds were evaluated. The initial cell adhesion area tended to be smaller on substrates with a higher amount of bound water. With further incubation, the hiPS-CMs formed self-pulsating aggregates on the substrate. On the substrates with high bound water content, the area of the hiPS-CMs aggregates tended to be smaller while the pulsation behavior became greater. The results indicate that PMEA analogues might affect the cellular properties of hiPS-CMs.

Key words: *iPS cell, Cardiomyocytes, PMEA analogues, Bound water, Intermediated water*

1. Introduction

Poly(2-methoxyethyl acrylate) (PMEA) is one of the biocompatible materials and has the property of inhibiting the deformation of proteins adsorbed on its surface.

PMEA weakly interacts with blood components and thus prevents the formation of blood clots.[1)] Due to the inertness of blood components, PMEA has been clinically applied as a coating material for blood-contacting medical devices.[2)] Previous studies have shown that PMEA analogues have "intermediate water" in the layer of water molecules adsorbed on the surface, and a correlation has been demonstrated between the amount of intermediate water and platelet adhesion inhibit ability.[3)] Further studies applying this property to the control of adhesive cell behavior suggested a correlation between cell adhesion force to PMEA analogues and the amount of bound water.[4-6)] In recent years, iPS cell-derived cardiomyocytes (hiPS-CMs) have attracted significant attention in the field of regenerative medicine. Numerous studies have been conducted and several problems have emerged, including the immaturity and low self-pulsatility of hiPS-CMs compared to adult human cardiomyocytes.[7)] Over the past few years, material properties affecting the maturity, self-pulsating force and function of hiPS-CMs have been investigated, for example, using decellularized plant-derived scaffolds and ECM-based scaffolds.[8-10)] However, few studies have examined the effects of scaffold surface properties on the pulsation behavior of hiPS-CMs. This study aimed to clarify the effect of PMEA analogues, which exhibit different cell adhesion properties depending on the amount of bound water, on the cellular properties of hiPS-CMs and identify the surface properties of materials that improve the self-pulsation behavior of hiPS-CMs.

*1 Department of Molecular and Material Sciences, Graduate Student
*2 Institute for Materials Chemistry and Engineering
*3 Department of Applied Chemistry, Graduate School of Engineering
*4 Research Institute for Applied Mechanics
*5 Department of Molecular and Material Sciences

2. Experimental

2.1 Preparation of polymer substrates

A solution of PMEA analogues was spin-coated on a biaxially oriented poly(ethylene terephthalate) (PET) sheet (DIAFOIL®T100E, Mitsubishi Chemical, Japan, thickness = 125 μm). First, substrates of the same size as the bottom of the 24-well culture plate (14 mm diameter) were cut from PET sheet using a laser cutter. In this study, all three PMEA analogues with different amounts of bound water, poly(2-methoxyethyl acrylate) (PMEA), poly(2-ethoxyethyl acrylate) (PEEA), and poly(2-methoxyethyl methacrylate) (PMEMA), were examined. The structural formula of the PMEA analogues are shown in Fig. 1. The polymers were synthesized using the same method as in our previous papers.[11] The molecular weight relative to standard polystyrene and the bound water content of each polymer are shown in Table 1.[6] Each polymer was dissolved in dehydrated toluene at a concentration of 0.5 wt/vol%, and all were filtered through a 0.20 μm pore size filter. 40 μl of PMEA analogue solution was applied to the PET substrate and coated using a spin coater (MS-A100, Mikasa Corp., Japan) at 3000 rpm for 40 seconds. Subsequently, the spin-coated substrates were dried under reduced pressure at 25 °C for 24 hours.

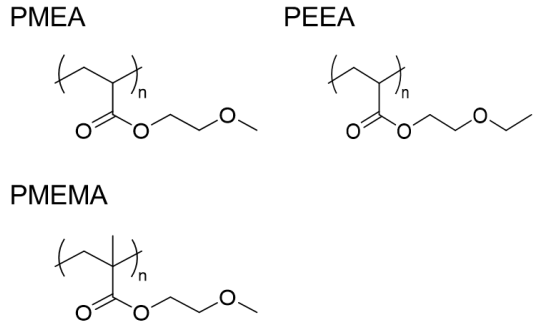

Fig. 1 Chemical structures of PMEA, PEEA, and PMEMA.

Table 1 Characteristics of PMEA analogous polymers.[6]

	Mn [g mol^{-1}]	Mw / Mn	Bound water [wt%]
PMEMA	91,000	2.09	2.3
PEEA	21,000	2.70	4.5
PMEA	29,000	2.82	6.2

2.2 Cell culture

Each substrate was UV-sterilized for 1 hour before seeding cells to prevent contamination. The hiPS-CMs (Carmy-A, Myoridge Co. Ltd., Japan), were pre-cultured for 7 days, and were seeded on each substrate at a density of 2.5 × 10^5 cells/well. PET substrates coated with PMEA analogous polymer were placed on the bottom of 24-well cell ultra-nonadherent multi-well plates (Costar® 24 Well Ultra Low Attachment Surface Flat Bottom Lid, Corning Inc.). The cells were then cultured in maintenance medium (Myoridge Co. Ltd., Japan) with continuous medium changes every 2 days.

2.3 Immunostaining

The cytoskeletal protein α-actinin was immunostained for evaluation of single-cell adhesion morphology of hiPS-CMs. The hiPS-CMs were seeded on each substrate at a low-density condition of 1.0 × 10^4 cells/well. 24 hours after seeding, hiPS-CMs were fixed with 4% PFA and cell nuclei were stained with 4',6-diamidino-2-phenylindole (DAPI). Mouse monoclonal anti-α-actinin (Sigma-Aldrich Inc.) was added as the primary antibody, and Alexa Fluor 488-conjugated anti-mouse IgG (H+L) the secondary antibody (Thermo Fisher Scientific Inc.) was added and incubated. After staining, the α-actinin and cell nuclei were observed by 10x objective lens using a confocal laser microscope (FV3000, Olympus Corp.). The captured image data were analyzed by an image processing software, ImageJ,[12] and cell area was measured.

2.4 Cell viability assay

The cell viability of hiPS-CMs on each substrate on the fifth day of culture was determined using a cell counting kit. After the cells were washed once with PBS, WST-8 solution (Cell Counting Kit, Dojindo Co., Ltd.) was added to each well and incubated at 37° C for 2 hours. The absorbance of the samples was measured by a plate reader (2030 ARVO X2, Perkin Elmer Co., Ltd.) at 450 nm.

2.5 Self-pulsating cell aggregate area

Video data of the self-pulsating hiPS-CMs aggregates on each substrate were captured using an inverted microscope (CKX53, Olympus Corp.). After 5 days of incubation, video data were captured at 40 fps for 20 seconds at 10 locations per well at ambient temperature. The captured video data were

analyzed as continuous image data by digital image correlation evaluation software, GOM Correlate2019,[13] to evaluate the displacement distribution (subset size: 9 pixels, distance between points: 4 pixels). The area of cell colonies showing localized pulsating in the displacement distribution map was measured using ImageJ image processing software.

2.6 Measurement of contraction behavior

The pulsation movie of the hiPS-CMs was analyzed for their pulsating behavior using repeated particle image velocimetry (PIV) in ImageJ.[14] An image before contraction and an image at the peak of contraction were selected from the continuous image data of the pulsating movie, and the displacement and direction associated with contraction were measured from the cross-correlation between the two images. The displacement behavior was obtained as displacement behavior in two axes, the X-axis and the Y-axis.

2.7 Statistical analysis

Data were calculated as the mean ± standard deviation of the results of at least three trials. Significant differences between means were assessed by the multiple comparison test Tukey HSD method using KaleidaGraph.[15] Statistical significance was set at * $P \leq 0.05$ and ** $P \leq 0.001$.

3. Results and discussion

3.1 Cell adhesion area

The adhesion area and morphology of single hiPS-CMs adhered to PMEA analogues were evaluated. Representative cell staining images of hiPS-CMs adhering to the substrates for α-actinin and cell nuclei are shown in Fig. 2. The results of measuring the cell adhesion area from the morphology image of α-actinin are also shown in Fig. 3. The higher amount of bound water content has the effect of decreasing of protein adsorption and inhibiting denaturation. Previous studies have shown that bound water content affects the adhesion morphology of cells that adhere via proteins.[16,17] The results of this study showed that cells on PMEA and PEEA substrates with relatively high bound water content tended to have a spherical cell morphology compared to PET and PMEMA. Furthermore, the cell adhesion area on PMEA and PEEA showed smaller compared to other substrates. The results observed in this study are consistent with previous reports and may be attributed to similar effects.[6]

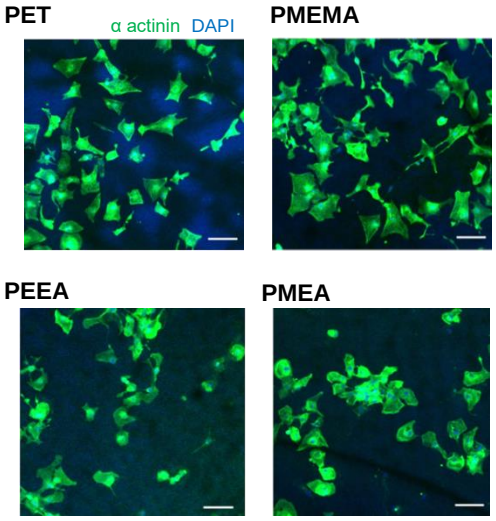

Fig. 2 The morphology of cell adhesion after 24 hours on each substrate. (scale bars : 100 μm)

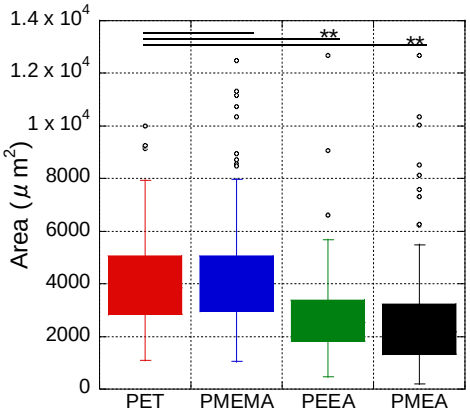

Fig. 3 Average cell adhesion area of single cells. (** P≦0.001)

3.2 Evaluation of pulsating colonies of hiPS-CMs

As the hiPS-CMs on the substrate, the cells began to show self-pulsation without any external stimuli. Continuous image data of the pulsating hiPS-CMs were analyzed by digital image correlation method, resulting in the displacement distribution shown in Fig. 4. On the substrates, deformation due to localized contraction of the hiPS-CMs was observed. Furthermore, it was observed that the sites of self-pulsation were highly consistent with the areas where cell aggregation and colonization took place on the substrate. The results of comparing the area of cell colonies that pulsating on each substrate are shown in Fig. 5. Cells on the PMEA and PEEA substrates showed a smaller cell aggregation area than PET and PMEMA, and showed a significant difference compared to cells on the PET substrate. The results of evaluating the cell viability of hiPS-CMs on the PMEA analogues on the fifth day of culture are shown in Fig. 6 and there was no significant difference in the number of adherent cells on each substrate. The results also suggested that adherent cells tended to aggregate more on PMEA and PEEA. This result is presumable because, on substrates with high bound water content, which have low cell adhesion properties, cell-to-cell binding forces exceed cell-to-substrate adhesion forces, resulting in migrating cells to be aggregated.[18,19]

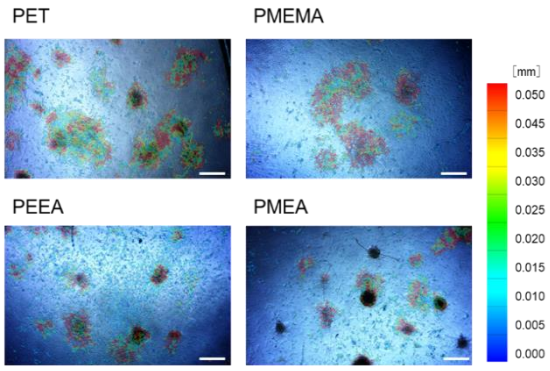

Fig. 4 Displacement distribution associated with contraction of hiPS-CMs aggregates analyzed by digital image correlation method. (scale bars :400 μm)

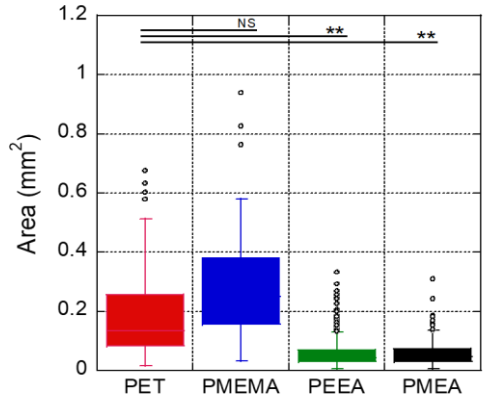

Fig. 5 Area of self- pulsating hiPS-CMs aggregates. (** P≦0.001) (n=3)

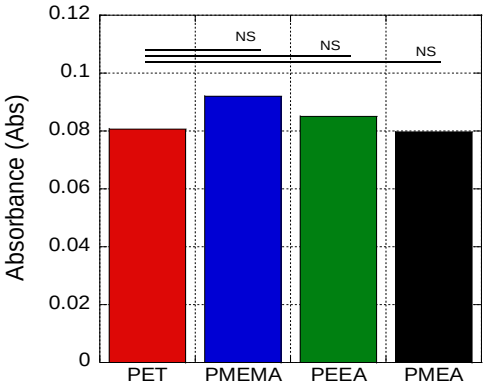

Fig. 6 Comparison of cell viability of hiPS-CMs cultured on the substrate of hiPS-CMs cultured on the substrate for 5 days. (n=3)

The self-pulsating force of the colony on the PMEA analogues was evaluated. The distribution of the magnitude of displacement and the direction of displacement associated with pulsation are shown in Fig. 7. In addition, the displacement behavior during contraction at each measurement point is shown in Fig. 8. The measurement position before contraction was defined as X = 0 μm and Y = 0 μm. Comparing the displacement behavior on each substrate, the hiPS-CMs colonies on PMEA in particular showed larger displacement behavior than those on the other substrates. Table 2 shows the results of a quantitative comparison of the pulsating behavior of hiPS-CMs on each substrate. Comparing the behavior of displacement caused by pulsation of hiPS-CMs colonies on each substrate, the percentage of points showing displacement of 5 μm or greater increased in the order of

PET<PMEMA<PEEA<PMEA. Furthermore, a comparison of the average displacement values with pulsation showed that the displacement of hiPS-CMs on the PMEA substrate was the largest and differed significantly from other substrates. Cardiomyocytes exhibit self-contractile capacity and excellent intercellular connectivity when adjacent cells are bound to each other and their aggregates are successfully developed organoids.[20] This suggests that since substrate-cell adhesion is low on substrates with high bound water content, the three-dimensional crowding of well-migrated cells may have resulted in cell aggregates with strong intercellular junctions exhibiting superior pulsation behavior.[21,22]

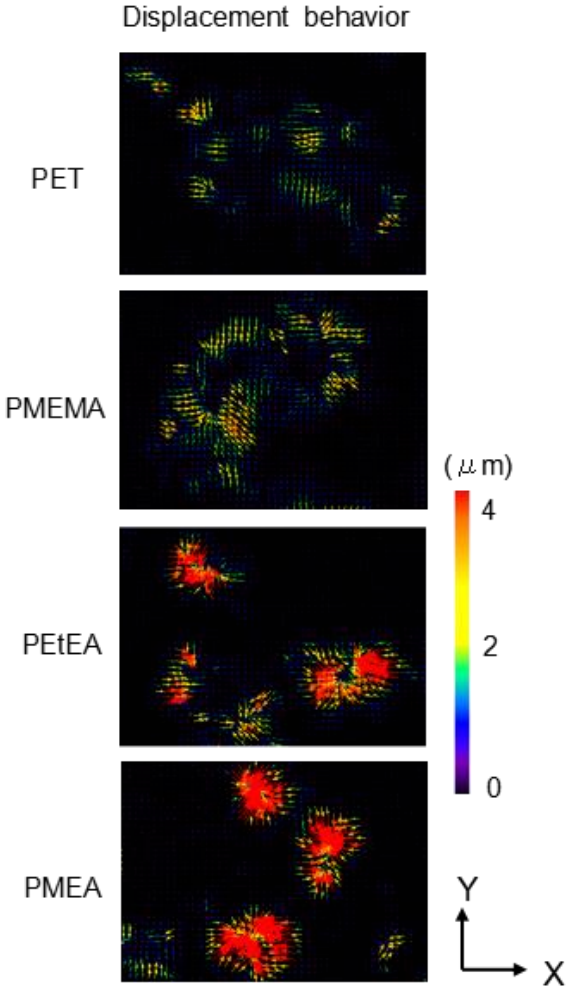

Fig. 7 Displacement maps of hiPS-CMs aggregates analyzed from two photographs before and after pulsation.

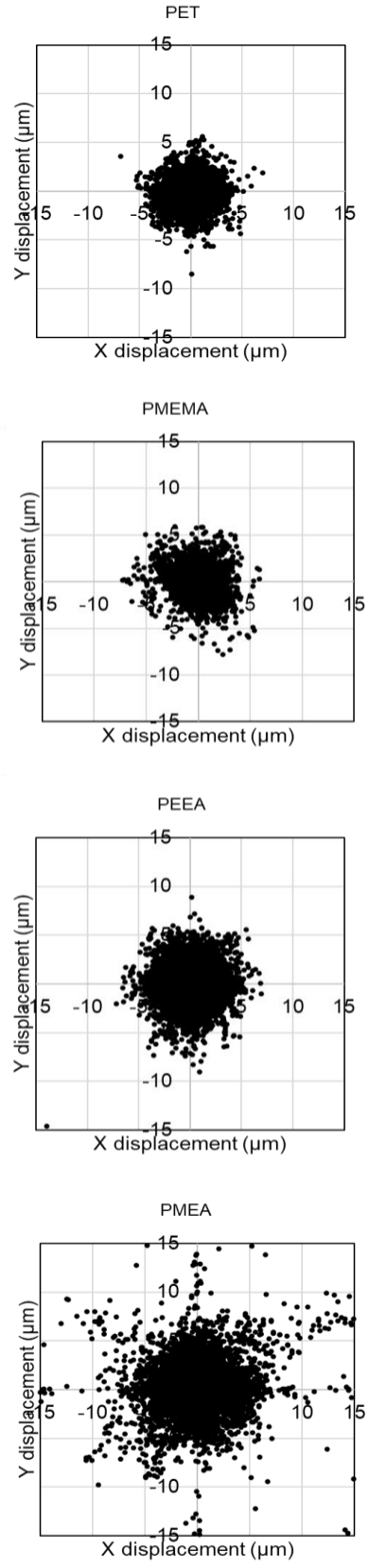

Fig. 8 Displacement behavior associated with pulsation of hiPS-CMs on substrate.

Table 2 Comparison of displacement behavior accompanying contraction. (n=3)

	Percentage of displacement behavior (5 μm~) (%)	Mean displacement with pulsation (μm)
PET	0.05	0.395
PMEMA	0.08	0.287
PEEA	0.21	0.393
PMEA	0.98	0.488

4. Conclusions

In this study, hiPS-CMs were cultured on PMEA analogues and the effect on hiPS-CMs was investigated. Substrates were prepared by coating biocompatible materials, PMEA analogues, on PET. The morphology of hiPS-CMs single cells was spherical morphology and the adhesion area was smaller, as the high content of binding water in the scaffold. The self-pulsating hiPS-CMs aggregates on the fifth day of culture were then evaluated. The results showed that the area of self-pulsating cell aggregates tended to be smaller on substrates with higher amounts of bound water. Furthermore, the magnitude of displacement associated with their self-pulsating was larger. Especially, hiPS-CMs cultured on PMEA showed significantly larger contraction behavior than others. This result suggests that the bound water content of scaffolds affects cell adhesion and weakens cell-scaffold interaction, resulting in stronger intercellular binding of cell aggregates and better self-contraction. In previous studies, cell alignment of hiPS-CMs with nanofiber scaffolds has been successful in expressing many genes related to intercellular junctions.[23] There was also an example of a study that succeeded in improving pulsation force by geometrically aggregating the hiPS-CMs by using Faraday waves.[22] This study demonstrated that hiPS-CMs exhibit different cell aggregation behaviors and different cellular characteristics when cultured on PMEA analogues with different amounts of bound water. In the future, it is expected to establish a scaffold material that can improve the pulsatility of hiPS-CMs by controlling the amount of bound water on the scaffold surface.

References

1) M. Tanaka, T. Motomura, M. Kawada, T. Anzai, Y. Kasori, T. Shiroya, K. Shimura, M. Onishi, A. Mochizuki, Biomaterials, 21, (2000), p. 1471-1481.
2) A. K. Zimmermann, H. Aebert, A. Reiz, M. Freitag, M. Husseini, G. Ziemer, H. P. Wendel, ASAIO j., 50, (2004), p. 193-199.
3) K. Sato, S. Kobayashi, M. Kusakari, S. Watahiki, M. Oikawa, T. Hoshiba, M. Tanaka, Macromol. Biosci., 15, (2015), p. 1296-1303.
4) T. Hoshiba, T. Otaki, E. Nemoto, H. Maruyama, M. Tanaka, ACS Appl. Mater. Interfaces, 7, (2015), p. 18096-18103.
5) M. A. Haque, D. Murakami, T. Anada, M. Tanaka, Coatings, 12, (2022), p. 1-16.
6) K. Nishida, T. Anada, S. Kobayashi, T. Ueda, M. Tanaka, Acta Biomater., 134, (2021), p. 313-324.
7) G. Kensah, A. R. Lara, J. Dahlmann, R. Zweigerdt, K. Schwanke, J. Hegermann, D. Skvorc, A. Gawol, A. Azizian, S. Wagner, L. S. Maier, A. Krause, G. Dräger, M. Ochs, A. Haverich, I. Gruh, U. Martin, Eur. Heart J., 34, (2013), p. 1134-1146.
8) E. R. Robbins, G. D. Pins, M. A. Laflamme, G. R. Gaudette, J. Biomed. Mater. Res. A, 108, (2020), p. 2123-2132.
9) S. S. Majidi, P. S. Adamsen, M. Hanif, Z. Zhang, Z. Wang, M. Chen, Int. J. Biol. Macromol., 118, (2018), p. 1648-1654.
10) Y. Efraim, B. Schoen, S. Zahran, T. Davidov, G. Vasilyev, L. Baruch, E. Zussman, M. Machluf, Sci. Rep., 9, (2019).
11) M. Tanaka, A. Mochizuki, J. Biomed. Mater. Res. A, 68A, (2004), p. 684-695.
12) J. Schindelin, C. T. Rueden, M. C. Hiner, K. W. Eliceiri, Mol. Reprod. Dev., 82, (2015), p. 518-529.
13) N. Soro, H. Attar, E. Brodie, M. Veidt, A. Molotnikov, M. S. Dargusch, J. Mech. Behav. Biomed. Mater., 97, (2019), p. 149-158.
14) T. Hayakawa, T. Kunihiro, T. Ando, S. Kobayashi, E. Matsui, H. Yada, Y. Kanda, J. Kurokawa, T. Furukawa, J. Mol. Cell., 77, (2014), p. 178-191.
15) E. Goto, F. Tokunaga, Biochem. Biophys. Res. Commun., 485, (2017), p. 152-159.
16) C. Sato, M. Aoki, M. Tanaka, Colloids Surf. B, 145, (2016), p 586-596.
17) T. Hoshiba, E. Nemoto, K. Sato, T. Orui, T. Otaki, A. Yoshihiro, M. Tanaka, PLOS ONE, 10, (2015), e0136066.
18) M. Y. Tsai, F. Aratsu, S. Sekida, S. Kobayashi, M. Tanaka, ACS Appl. Bio Mater., 3, (2020), p. 1858-1864.
19) K. Nishida, S. Sekida, T. Anada, M. Tanaka, ACS Biomater. Sci. Eng., 8, (2022), p. 672-681.
20) R. K. Iyer, L. L. Y. Chiu, M. Radisic, J. Biomed. Mater. Res., 89A, (2009), p. 616-631.
21) N. J. Daily, Y. Yin, P. Kemanli, B. Ip, T. Wakatsuki, J. Bioeng Biomed Sci., 5, (2015), p. 1-10.
22) V. Serpooshan, P. Chen, H. Wu, S. Lee, A. Sharma, A. D. Hu, S. Venkatraman, V. A. Ganesan, O. B. Usta, M. Yarmush, F. Yang, C. J. Wu, U. Demirci, M. S. Wu, Biomaterials, 131, (2017), p. 45-57.
23) M. Khan, Y. Xu, S. Hua, J. Johnson, A. Belevych, P. M. L. Janssen, S. Gyorke, J. Guan, M. G. Angelos, PLOS ONE, 10, (2015), p. 1-19.